

Noninteracting Dark Matter

P. J. E. Peebles

Institute for Advanced Study, Princeton NJ 08540

and

A. Vilenkin

Institute of Cosmology,

Department of Physics, Tufts University, Medford MA 02155

(April 26, 2024)

Abstract

Since an acceptable dark matter candidate may interact only weakly with ordinary matter and radiation, it is of interest to consider the limiting case where the dark matter interacts only with gravity and itself, the matter originating by the gravitational particle production at the end of inflation. We use the bounds on the present dark mass density and the measured large-scale fluctuations in the thermal cosmic background radiation to constrain the two parameters in a self-interaction potential that is a sum of quadratic and quartic terms in a single scalar dark matter field that is minimally coupled to gravity. In quintessential inflation, where the temperature at the end of inflation is relatively low, the field starts acting like cold dark matter relatively late, shortly before the epoch of equal mass densities in matter and radiation. This could have observable consequences for galaxy formation. We respond to recent criticisms of the quintessential inflation scenario, since these issues also apply to elements of the noninteracting dark matter picture.

I. INTRODUCTION

We have improving observational evidence [1] on how structure formed on the scale of galaxies and larger from measurements of the angular distributions of the radiation backgrounds, surveys of the spatial distributions and motions of the galaxies, and observations of the evolution of galaxies and the intergalactic medium back to redshift $z \sim 5$. It may prove useful to complement these advances with explorations of the options conventional physics offers for theories of structure formation. Here we consider the possibility that the dark matter that is thought to dominate the gravitational growth of structure interacts only with itself and gravity, the dark matter originating by gravitational particle production, that is, as a squeezed state, at the end of inflation.¹

¹Such dark matter particles might be called cabots, in honour of the Cabot family of Boston, who were said to be so highly placed in society as to speak only to God.

After specifying our model in Section II, we discuss the state of the dark matter field at the end of inflation. We begin in Section III with the equilibrium properties of a noninteracting dark mass scalar field in de Sitter spacetime. For many purposes de Sitter spacetime is a useful approximation to inflation, and it has the particular advantage that the equilibrium statistical properties of the dark mass field are well specified [2–4]. However, it is also of interest to analyze the effect of the rolling value of the Hubble parameter in a model for the relatively late stages of inflation. This is presented in Section IV, following in part the early work by Kofman and Linde [5]. Section V deals with the constraints on the mass of the dark matter particles and on their self-coupling from the conditions that a single scalar field has the wanted present mean mass density and field fluctuations that are compatible with the large-scale anisotropy of the thermal background. In quintessential inflation [6] this dark matter candidate has an observationally interesting effective Jeans length.

We discuss in section VI issues of internal consistency of the model. In a recent preprint Felder, Kofman and Linde [7] have presented a stimulating list of potential problems with quintessential inflation and indirectly with the noninteracting dark matter model. We address their points in this section. An assessment of consistency with the full suite of observational tests requires computations that go well beyond our exploratory discussion; we also comment on these open issues in Section VI.

II. ASSUMPTIONS

The dark matter is modeled as a single scalar field, $y(\mathbf{x}, t)$, that is minimally coupled to gravity and has the self-interaction potential

$$V = \lambda y^4/4 + \mu^2 y^2/2. \quad (1)$$

The generalization to several field components with $O(N)$ symmetry and the opposite sign of the quadratic part of the potential is trivial and not interesting for the present purpose.

We assume that there is a time before the end of inflation when the Hubble parameter $H(t)$ is close enough to constant that the dark matter field can relax to near statistical equilibrium between the amplitude growth driven by quantum fluctuations and the classical slow roll due to the self-interaction potential, in an approximation to a de Sitter-invariant quantum state. For definiteness, much of our discussion of this assumption is based on a quartic inflaton potential,

$$U = \lambda_\phi \phi^4/4, \quad (2)$$

with a self-coupling satisfying $\lambda_\phi \lesssim 10^{-14}$, for consistency with the isotropy of the thermal cosmic background radiation (the CBR). Kofman and Linde [5] consider the two-field model in Eqs (1) and (2) in the limit where the evolution of y is essentially classical. Following their methods in part, we show in Section VI that, when

$$\lambda \gg \lambda_\phi, \quad (3)$$

the y -field energy density indeed remains subdominant during inflation, as required for internal consistency. We show in Section V that the condition (3) is within the ranges of values of λ and λ_ϕ allowed by the CBR.

We assume the mass parameter μ is small enough that the quartic part of the potential dominates during inflation, that λ is small enough that the field may be approximated as the sum of a classical part and a free quantum field, and that radiative corrections to the potential in Eq. (1) are negligible. The condition for the last assumption is [8]

$$\frac{3\lambda}{64\pi^2} \ln \frac{1}{\lambda} \ll 1. \quad (4)$$

We use a homogeneous cosmological model in which the field equation is

$$\frac{\partial^2 y}{\partial t^2} + 3\frac{\dot{a}}{a} \frac{\partial y}{\partial t} = \frac{\nabla^2 y}{a^2} - (\lambda y^2 + \mu^2)y. \quad (5)$$

For $\lambda y^2 \ll H^2$, the oscillation frequency due to the quartic part of the potential is small compared to H , and we can use the slow roll approximation to the field equation,

$$3H\partial y/\partial t = -\lambda y^3. \quad (6)$$

This neglects the mass term, which is justified for $y^2 \gg \mu^2/\lambda$.

We consider both the conventional model for reheating and the much lower temperature at the end of inflation implied by the quintessential inflation model [6]. In the latter case the mass density in interacting matter at the end of inflation is proportional to the fourth power of the Hubble parameter, with a coefficient that depends on the nature of the matter and its interactions. We comment on the uncertainty in this coefficient in Section VI.

We write the Planck mass as $m_{\text{pl}} = [3/(8\pi G)]^{1/2}$ in units where $\hbar = 1 = c$. The Hubble parameter during inflation is H and the value at the end of inflation is H_x . In section V the present value of Hubble's constant is $H_o = 100h \text{ km s}^{-1} \text{ Mpc}^{-1}$. Numerical examples assume $h = 0.7$, density parameter $\Omega_m = 0.3$ in matter capable of clustering, and a cosmologically flat universe.

III. STATISTICS OF THE MATTER FIELD IN DE SITTER SPACETIME

On scales larger than the de Sitter horizon, H^{-1} , the dynamics of the field y can be pictured as a ‘‘random walk’’ [superimposed on the classical slow roll in Eq. (6)] in which y undergoes random steps of rms magnitude $(\delta y)_{\text{rms}} = H/2\pi$ per expansion time $\delta t = H^{-1}$, independently in each horizon-size region. The statistical properties of the field y resulting from this random process can be described in terms of the probability distribution function $P(y, t)$ which satisfies the Fokker-Planck equation [2,3]

$$\frac{\partial P(y, t)}{\partial t} = \frac{1}{3H} \frac{\partial}{\partial y} [V'(y)P(y, t)] + \frac{H^3}{8\pi^2} \frac{\partial^2 P(y, t)}{\partial y^2}. \quad (7)$$

Any initial distribution, $P(y, 0)$, approaches the stationary solution of (7),

$$P_0(y) = N^{-1} \exp\left(-\frac{8\pi^2}{3H^4} V(y)\right), \quad (8)$$

on the timescale [4]

$$\tau_{\text{rel}} \sim \lambda^{-1/2} H^{-1}. \quad (9)$$

The coefficient N in (8) is determined from the normalization condition $\int_{-\infty}^{\infty} P_0(y) dy = 1$. The stationary distribution $P_0(y)$ corresponds to the de Sitter-invariant quantum state of the field y . The statistical properties of this state in the case of a quartic potential $V(y) = \lambda y^4/4$ have been studied by Starobinsky and Yokoyama [4] (hereafter SY).

The distribution function $P_0(y)$ is not Gaussian; in particular it has negative excess kurtosis [4] $\langle \phi^4 \rangle / (\langle \phi^2 \rangle)^2 - 3 \approx 0.812$. In the following numerical example of correlation functions of powers of the field, we will refer to the moments

$$\begin{aligned} \langle y^2 \rangle &= 0.1318 H^2 \lambda^{-1/2}, & \langle y^4 \rangle - \langle y^2 \rangle^2 &= 0.0206 H^4 \lambda^{-1}, \\ \langle y^6 \rangle &= 0.01502 H^6 \lambda^{-3/2}, & \langle y^8 \rangle - \langle y^4 \rangle^2 &= 0.00577 H^8 \lambda^{-2}, \\ \langle y^{12} \rangle - 3 \langle y^4 \rangle \langle y^8 \rangle + 2 \langle y^4 \rangle^3 &= 0.001755 H^{12} \lambda^{-3}. \end{aligned} \quad (10)$$

SY use the Fokker-Planck formalism to compute the field correlation function $\langle y_1 y_2 \rangle$. Their method and numerical results are readily adapted to get the correlation function of powers of the field, in particular the correlation function of the mass density $\lambda y^4/4$. This is done in the Appendix; we find that for a positive integer power n of the field the equal time reduced correlation function of y^n at large separation x_{12} is

$$c_n(x_{12}) = \langle y_1^n y_2^n \rangle - \langle y^n \rangle^2 \propto x_{12}^{-p}, \quad (11)$$

where the power law index is

$$p = 0.178 \lambda^{1/2} \quad (\text{odd } n), \quad p = 0.579 \lambda^{1/2} \quad (\text{even } n). \quad (12)$$

The power law in Eq. (11) applies at separations large compared to the comoving coherence length

$$R_c = (aH)^{-1} \exp(1/p) \sim (aH)^{-1} e^{\alpha H \tau_{\text{rel}}}, \quad (13)$$

with the appropriate value of p from Eq. (12), and where α is a number of order unity. This expression can be interpreted to mean that in the relaxation time τ_{rel} (Eq. 9) comoving positions initially separated by the Hubble length have moved to separation aR_c , with significant loss of memory of the common initial field values at the two positions.

As an alternative to the Fokker-Planck formalism, it may be convenient to use a discrete version of the Langevin equation. In an expansion time, $t = H^{-1}$, the value of the field y at a fixed comoving position changes by the amount

$$y(j) \rightarrow y(j+1) = y(j) - \lambda y(j)^3 / (3H^2) + \iota_j H / (2\pi). \quad (14)$$

The integer j counts successive expansion times H^{-1} . The Gaussian normal random variables ι_j have zero mean and are statistically independent, so in particular $\langle \iota_j \iota_k \rangle = \delta_{j,k}$. The second term on the right-hand side of Eq. (14), which represents the classical force due to the potential that tends to drive y toward zero, follows from the slow roll approximation in Eq. (6). The last term represents the frozen quantum fluctuations added to y in the expansion time H^{-1} .

In the stationary de Sitter-invariant state, the mean square value of y is independent of time. This condition applied to Eq. (14), and keeping first powers of the classical drift part and second powers of the fluctuating part, yields the mean mass density in the y -field,

$$\langle \rho_y \rangle = \lambda \langle y^4 \rangle / 4 = 3H^4 / (32\pi^2). \quad (15)$$

The condition $\langle y(j)^6 \rangle = \langle y(j+1)^6 \rangle$ similarly yields

$$\langle y^8 \rangle / \langle y^4 \rangle^2 = 5. \quad (16)$$

These relations agree with the Fokker-Planck results given above, as expected. Eq. (16) says the standard deviation of the frozen field mass fluctuations is $\delta\rho/\rho = 2$, with coherence length $R_c \sim H^{-1} \exp(1.7\lambda^{-1/2})$.

Eq. (14) may be applied as a numerical iteration prescription, where the integers j count iterations and the numbers ι_j are drawn from a generator of pseudo-Gaussian independent random numbers with zero mean and unit variance. We use it to calculate the two-point functions (11) and illustrate the different power law indices for even and odd n . The computation starts with an initial value $y(0)$ obtained after 300 iterations of Eq. (14) starting from $y = 0$. Two time series, $y_1(j)$ and $y_2(j)$, are computed from the same initial value $y(0)$ and different sets of the ι_j . This is a numerical realization of the values of the y -field at successive expansion times H^{-1} at two fixed comoving positions that are separated by the Hubble length at $j = 0$. A set of realizations is obtained by using the last value of the time series y_1 as the initial value for the next realization of $y_1(j)$ and $y_2(j)$. The mean of $y_1^n(j)y_2^n(j)$ across a set of these realizations is an estimate of the expectation value $\langle y_1^n y_2^n \rangle$ at separation $x_{12} \propto e^j$.

Fig. 1 shows numerical results for $n = 1, 2, 3$, and 4 in Eq. (11). The variables are scaled to

$$\hat{c}_n = \lambda^{n/2} H^{-2n} c_n, \quad \hat{x}_{12} = (Hax_{12})^{\sqrt{\lambda}}, \quad (17)$$

to remove the dependence on the parameters H and λ at zero separation (Eq. 10) and at large separation (Eq. 12). The heavy lines in the figure are the averages across realizations for two parameter choices, $\lambda = 0.1$ and $\lambda = 0.0001$. The latter requires a much larger number of iterations to reach a given range of values of the correlation functions. That reduces the number of realizations in the computation, so the numerical noise is larger. The straight dotted lines are interpolations based on the SY results: the intercepts at zero separation are the one-point moments in Eq. (10) and the slopes are the power law indices 0.178 and 0.579 for the scaled variable $(Hax)^{\sqrt{\lambda}}$ (Eq. 12). Within the fluctuations from the limited number of realizations in the averages (1×10^8 for $\lambda = 0.1$ and 1×10^7 for $\lambda = 1 \times 10^{-4}$) the numerical estimates are consistent with the expected scaling with λ . Since the power-law asymptotics apply only for $x > R_c$, one could not expect them to match with the one-point moments which correspond to $ax \sim H^{-1} \ll aR_c$. Fig. 1 indicates, however, that the difference from a pure power law is not dramatic: the mismatch is no more than a factor of about 2.

The lowest curves in Fig. 1 show the mass correlation function $\xi(x_{12}) \propto \langle y_1^4 y_2^4 \rangle - \langle y^4 \rangle^2$. At large separation the numerical result is a factor of about two below the extrapolation from zero separation. Since the reduced second moment of the mass distribution is $\xi = 4$ at

zero separation (Eq. 16), a useful approximation to the dimensionless dark mass correlation function is

$$\xi(x) = \langle \delta_1 \delta_2 \rangle \sim 2(x_x/x)^\epsilon, \quad \epsilon = 0.58\lambda^{1/2}, \quad (18)$$

where x_x is the comoving Hubble length at the end of inflation and the density contrast is

$$\delta = \rho/\langle \rho \rangle - 1 = y^4/\langle y^4 \rangle - 1. \quad (19)$$

Comparison to the moments of large-scale fluctuations in the counts of galaxies [10] requires higher moments of the y -matter distribution; we present the example of the three-point function. The reduced dimensionless three-point mass correlation function is

$$\begin{aligned} \xi_3 &= \langle \delta_1 \delta_2 \delta_3 \rangle \\ &= \langle y_1^4 y_2^4 y_3^4 \rangle / \langle y^4 \rangle^3 - (\langle y_1^4 y_2^4 \rangle + \langle y_2^4 y_3^4 \rangle + \langle y_3^4 y_1^4 \rangle) / \langle y^4 \rangle^2 + 2. \end{aligned} \quad (20)$$

The arguments of ξ_3 are the lengths of the sides of the triangle defined by the positions at which the field is evaluated. It is shown in the Appendix that if the three points define an equilateral triangle with side x much larger than R_c then the three-point function varies with x as $\xi_3 \propto \xi^{3/2}$, where the two-point function ξ (Eq. 18) is evaluated at x . The one-point moments (Eq. 10) show that $\xi_3/\xi^{3/2} = 4$ at zero separation.

Fig. 2 shows numerical realizations of $\xi_3/\xi^{3/2}$ for equilateral triangles. The estimates of ξ_3 are based on sets of three independent time series $y_1(j)$, $y_2(j)$, and $y_3(j)$ with the same initial value. The values of λ , the numbers of realizations, and the scaled variables are the same as for Fig. 1. The curves are close to the SY one-point moments at small separation, and, as also predicted by the Fokker-Planck method, at scaled separation $\hat{x} \gtrsim 10$ the ratio is close to independent of triangle size, within the considerable noise from the limited number of realizations, at

$$\xi_3/\xi^{3/2} \simeq 0.8 \quad (21)$$

This gives a useful working approximation to the normalization of the three-point function on scales of interest for structure formation.²

The scaling of the n -point mass correlation functions with distance x at fixed values of the ratios x_{ij}/x_{kl} of distances among the n points may be obtained by the following argument. Let $\bar{\delta}_i = \delta\rho/\rho$ be the mass density contrast at expansion parameter $a = a_i$ smoothed within a window of fixed comoving size, shape, and position, and let $\bar{\delta}_f$ be the density contrast smoothed in the same window at a later time, at expansion parameter a_f . A realization $\delta(t)$ of the evolution from δ_i to δ_f is a result of the process of freezing of quantum fluctuations and the classical evolution toward $\delta = 0$. If a_f/a_i is large enough that the epochs are separated by many relaxation times, the initial value δ_i is a small perturbation to this process, and

²The asymptotic value of the ratio in Eq. (21) can be found by a numerical computation of the eigenfunction $\Phi_2(y)$ and the integral C in Eq. (110) of the Appendix. We have not attempted this computation.

in the lowest nontrivial order in perturbation theory the expectation value of $\bar{\delta}_f$ for given initial value $\bar{\delta}_i$ is linear in $\bar{\delta}_i$:

$$\langle \bar{\delta}_f \rangle_{\bar{\delta}_i} = T \bar{\delta}_i. \quad (22)$$

The transfer coefficient T is a function of the window size and shape, which we are holding fixed in comoving coordinates, and of the expansion factor a_f/a_i , which we will vary. Next we consider two disjoint windows, both of fixed size, shape and position in the same comoving coordinate system. If the distance between the windows is much larger than the Hubble length at a_i the evolution of the density contrast in window 1 is independent of the process in window 2, and it follows that the equal time mass two-point correlation function satisfies

$$\langle \bar{\delta}_f(1) \bar{\delta}_f(2) \rangle = T^2 \langle \bar{\delta}_i(1) \bar{\delta}_i(2) \rangle. \quad (23)$$

In the de Sitter equilibrium state the two-point mass correlation function depends only on the proper separation ax , so we can rewrite Eq. (23) as

$$\xi(bx) = T(b)^2 \xi(x), \quad b = a_f/a_i. \quad (24)$$

This implies

$$\xi \propto x^{-2\nu}, \quad T \propto b^{-\nu}, \quad (25)$$

where ν is a constant that must be positive for convergence. That is, at large separation x the correlation function varies as a power of x , as was shown more directly by our use of the SY analysis. The n -point function similarly satisfies

$$\langle \bar{\delta}_f(1) \dots \bar{\delta}_f(n) \rangle = T^n \langle \bar{\delta}_i(1) \dots \bar{\delta}_i(n) \rangle, \quad (26)$$

from which it follows that the n -point function scales with the separation x at fixed ratios of separations among the n points as

$$\xi_n \propto x^{-n\nu}, \quad (27)$$

consistent with Eq. (21).

Eq. (27) says the n^{th} central moment of the dark mass M contained in a volume of fixed shape scales as $M_n = \langle (M - \langle M \rangle)^n \rangle \propto \sigma^n$, where $\sigma = (\langle (M - \langle M \rangle)^2 \rangle)^{1/2}$ is the standard deviation (and assuming the integrals over the correlation functions converge at vanishing separation between points). The smoothed mass fluctuations do not approach a Gaussian as the size of the smoothing window is increased. Rather, this is a scale-invariant fractal in which the mass fluctuations smoothed and referred to the standard deviation are independent of the size of the smoothing window.

IV. THE DARK MATTER AT THE END OF INFLATION

We have assumed so far that the evolution of the inflaton ϕ is sufficiently slow that the field y has enough time to settle into its de Sitter-invariant “equilibrium” state. Here we specify the conditions of applicability of this picture under a specific inflaton potential, and

we consider the transition to the opposite regime, which applies toward the end of inflation, when the evolution of y is almost classical.

For the inflaton potential in Eq. (2) an approximate solution for the expansion history through inflation is [11]

$$H = H_x e^{-H_x t}, \quad H_x = \frac{4}{3} \lambda_\phi^{1/2} m_{\text{pl}}, \quad \phi_x = (8/3)^{1/2} m_{\text{pl}}, \quad (28)$$

with expansion parameter

$$\log a_x/a = H/H_x - 1. \quad (29)$$

We write the comoving length scale x of field fluctuations frozen at time t , when the expansion and Hubble parameters are a and H , as

$$Hax = 1. \quad (30)$$

This comoving length reaches its minimum value, x_x , at the end of inflation. In Eq. (28) inflation ends at $t = 0$, when the Hubble parameter and inflaton field values are H_x and ϕ_x .

In the approximation of Eqs. (28) to (30) the Hubble parameter H when the field fluctuations on the comoving length scale x are freezing satisfies

$$\log(x/x_x) \simeq \log(H_x/H) + H/H_x - 1. \quad (31)$$

A useful approximation at $a \ll a_x$ is

$$x/x_x \sim e^{H/H_x}. \quad (32)$$

The relaxation time for y and the evolution time for H are (Eqs. 9 and 28)

$$\tau_{\text{rel}} \sim \lambda^{-1/2} H^{-1}, \quad \tau_H \sim H_x^{-1}. \quad (33)$$

When $\tau_{\text{rel}} \ll \tau_H$ the y -field relaxes to statistical equilibrium between fluctuations and classical slow roll, in a good approximation to the de Sitter equilibrium state. When $\tau_{\text{rel}} \gg \tau_H$ the field evolution is close to classical. At the transition between these limiting cases, at expansion parameter a_e , the Hubble parameter is

$$H_e \sim \lambda^{-1/2} H_x. \quad (34)$$

Since the y -field at $a = a_e$ is close to statistical equilibrium its characteristic value is $y_e \sim \lambda^{-1/4} H_e$ (Eq. 10). This is related to the value of the inflaton at $a = a_e$ by

$$y_e/\phi_e \sim (\lambda_\phi/\lambda)^{1/2}. \quad (35)$$

Kofman and Linde [5] show that, if the inflaton and the y -field both have quartic potentials, the evolution in the slow roll classical approximation is

$$(\lambda_\phi \phi^2)^{-1} - (\lambda y^2)^{-1} = \text{constant} = (\lambda_\phi \phi_x^2)^{-1} - (\lambda y_x^2)^{-1}. \quad (36)$$

Eq. (35) says the constant of integration is not very important at $a = a_e$, so a good approximation to the smaller field values at $a_e \ll a \lesssim a_x$ is

$$y(t) = (\lambda_\phi/\lambda)^{1/2}\phi(t). \quad (37)$$

We consider first the field fluctuations frozen at $a_e < a < a_x$, when the evolution of y is close to classical. In unit logarithmic interval of x the contribution to the variance of the frozen dark mass field is $\delta y_x^2 = (H/2\pi)^2$. Apart from regions where y happens to be close to zero, this is a small fractional perturbation to the field value. With Eqs. (36) and (37) we see that the field perturbation at the end of inflation is³

$$\frac{\delta y_x}{y_x} = \frac{\delta y}{y} \left(\frac{y_x}{y}\right)^2 = \frac{H}{2\pi\phi_x} \left(\frac{\phi_x}{\phi}\right)^3 \left(\frac{\lambda}{\lambda_x}\right)^{1/2}. \quad (38)$$

Here H , y , and ϕ are evaluated when field fluctuations on the scale x are frozen, at $\log(x/x_x) = (\phi/\phi_x)^2$ in the approximation of Eq. (32). With Eq. (28) we get

$$\delta y_x/y_x \sim 0.1\lambda^{1/2}[\log(x/x_x)]^{-1/2}. \quad (39)$$

Since this is nearly independent of the length scale x the power spectrum varies with wave number about as k^{-3} , and the mass correlation function is

$$\xi \sim M\lambda \log(x_e/x), \quad (40)$$

where M is a dimensionless constant.

At separations larger than the field coherence length, $R_c \sim (a_e H_e)^{-1} \exp(1/p)$ with $p \sim \lambda^{1/2}$ (Eq. 12), Eq. (40) fails; the values y_e may be quite different at the two points. The classical evolution Eq. (36) says the field values at a given comoving position $a = a_e$ and at the end of inflation at $a = a_x$ satisfy

$$\frac{1}{y_x^2} = \frac{1}{y_e^2} + \frac{\lambda}{H_x^2}(1 - \sqrt{\lambda}). \quad (41)$$

If $\lambda \ll 1$ this says the field value is $y_x \sim \pm\lambda^{-1/2}H_x$ everywhere except near the surfaces where y_e vanishes, and the energy density is

$$\rho_x \sim \lambda^{-1}H_x^4, \quad (42)$$

except near the zeros of y_e . If the distance between zeros were larger than the typical motion of the dark mass after inflation the present distribution would be close to uniform apart from surfaces of low density.

We estimate the form of the mass correlation function at the end of inflation and for separation $x \gg R_c$ by the argument used to obtain the scaling of the n -point mass correlation functions in the de Sitter-invariant case in Eq. (27). Consider two windows with fixed sizes and positions in comoving coordinates. The dark mass density contrasts smoothed within

³To avoid confusion we remind the reader that $\delta y_x/y_x$ is the fractional fluctuation in the dark matter field value at the end of inflation. The subscript x in Eq. (38) has nothing to do with the comoving length scale of the fluctuation in Eq. (39).

these windows are $\bar{\delta}_e(1)$ and $\bar{\delta}_e(2)$ at expansion parameter $a = a_e$, when the field fluctuations start to depart from the de Sitter-invariant state, and $\bar{\delta}_x(1)$ and $\bar{\delta}_x(2)$ at the end of inflation at $a = a_x$. If the comoving separation $a_e x_{12}$ of the windows is large compared to R_c at a_e then we have, following the derivation of Eq. (25),

$$\langle \bar{\delta}_x(1) \bar{\delta}_x(2) \rangle = T^2 \langle \bar{\delta}_e(1) \bar{\delta}_e(2) \rangle \sim N(x_x/x_{12})^{0.6\sqrt{\lambda}} \sim \xi_x(x_{12}). \quad (43)$$

The power law coefficient follows from the de Sitter-invariant correlation function (18). The transfer coefficient T , defined as in Eq. (22), depends on λ . In general it also depends on the window size and shape, but in the limit where the two windows are small compared to their separation Eq (43) reduces to the two-point mass correlation function.

Quite similarly, the three-point mass correlation function satisfies

$$\langle \bar{\delta}(1) \bar{\delta}_x(2) \bar{\delta}_x(3) \rangle = T^3 \langle \bar{\delta}_e(1) \bar{\delta}_e(2) \bar{\delta}_e(3) \rangle. \quad (44)$$

Combined with Eq.(43) this implies that the relation (21) between the three- and two-point correlation functions is still valid at the end of inflation.

If λ is not much smaller than unity the near de Sitter evolution ends not long before the end of inflation. In this case an estimate of the mass correlation function at the end of inflation from a numerical realization of the process is easy and useful. As in Section II, we label successive e-foldings of the comoving Hubble length by the integer j , but now j decreases with time, with $j = 1$ at the end of inflation. The values of the Hubble constant follow from Eq (31),

$$e^{j-1} = \frac{x_j}{x_x} = \frac{e^{H_j/H_x - 1}}{H_j/H_x}. \quad (45)$$

Eq. (36) says the values of the dark matter and inflation fields at successive e-foldings are related by

$$\frac{1}{\lambda} \left(\frac{1}{y_j^2} - \frac{1}{y_{j+1}^2} \right) = \frac{1}{\lambda_\phi} \left(\frac{1}{\phi_j^2} - \frac{1}{\phi_{j+1}^2} \right). \quad (46)$$

The result of multiplying this by H_x^2 , rearranging, and adding the quantum noise term $\pm H/(2\pi)$ at each e-folding of x is

$$z_j = \frac{z_{j+1}}{[1 + G_j z_{j+1}^2]^{1/2}} + \frac{\nu_j h_j}{2\pi}, \quad (47)$$

where the ν_j are independent Gaussian normal numbers, the field has been scaled to

$$z = y/H_x, \quad (48)$$

and

$$G_j = \frac{2\lambda}{3} \left(\frac{H_x}{H_j} - \frac{H_x}{H_{j+1}} \right). \quad (49)$$

The H_j come from the numerical solution of Eq. (45). The two-point function at separation $x/x_x = e^j$ is the mean of products of field values computed starting from a common value j time steps before the end of inflation.

Figure 3 compares the mass correlation functions at the end of inflation for constant Hubble parameter and for the rolling case in Eq. (28), for $\lambda = 0.1$. One sees that at relatively small separations $\xi(x)$ is considerably flatter in the rolling H case, as expected from Eq (40). The values and rates of change of the correlation functions are roughly similar at separations $x \sim 10^{15}x_x$. This suggests that for $\lambda = 0.1$ the constant N in Eq. (43) is not greatly different from unity.

At smaller λ a numerical realization of the two-point function is difficult because the relaxation time is long, but it is easy to get the one-point distribution of y at the end of inflation. At $\lambda = 0.001$ the distribution is strongly peaked at $y \sim \pm\lambda^{-1/2}H_x$, as expected (Eq. 42), but there is significant scatter from the quantum fluctuations appearing at $a \lesssim a_e$. For $\lambda = 0.1$ the distribution of field values y is peaked at zero, and not greatly different from the stationary de Sitter case.

In the next section we use the estimates of the field mass fluctuations in Eqs. (39) and (43) with the measured CBR anisotropy to find bounds on the parameter λ . We will argue that the considerable uncertainty in N translates to a relatively small uncertainty in the bound on λ .

V. THE DARK MATTER AT THE PRESENT EPOCH

We consider three constraints: the present mean mass density in dark matter, the small-scale cutoff in the gravitational growth of clustering of the y -matter, and the large-scale anisotropy of the thermal background radiation. Because most of our estimates are quite approximate we ignore most numerical factors that are of order unity.

A. The Mean Mass Density

With the change from proper world time t to conformal time $x^0 = \int dt/a$, and the definition $\tilde{y} = ay$, the action for the y -field is

$$S = \int d^4x \left(\frac{1}{2} \tilde{y}_{,i} \tilde{y}^{,i} - \frac{1}{4} \lambda \tilde{y}^4 - \frac{1}{12} a^2 \tilde{y}^2 R \right), \quad (50)$$

where the index is raised by the Minkowski metric tensor and we ignore the quadratic part of the potential. The Ricci tensor R is on the order of the square of the Hubble parameter \dot{a}/a when the universe is matter-dominated, and it is well below that when radiation-dominated. When the Ricci term may be neglected a solution for \tilde{y} in Minkowski spacetime is a solution for ay expressed as a function of comoving coordinates and conformal time. The y -field energy density depends on the proper time derivative $\dot{y} = (\partial\tilde{y}/\partial x^0 - \tilde{y}\dot{a})/a^2$. If the field oscillates rapidly on the scale of the Hubble time, either because the potential is driving rapid oscillations or the field varies with position on scales small compared to the Hubble length, then $\dot{y} = a^{-2}\partial\tilde{y}/\partial x^0$ to good accuracy, and the proper field energy density is well approximated as the energy density of \tilde{y} in Minkowski coordinates divided by a^4 . Since the former conserves energy the mean energy density in the y -field varies as

$$\rho_y \propto a^{-4}. \quad (51)$$

The characteristic amplitude of the field oscillations thus scales as

$$y \propto 1/a(t). \quad (52)$$

Ford [12] obtained these results for a quartic potential when y is a function only of world time. It is an easy exercise to obtain Eqs (51) and (52) by extending Ford's method to the case where the scales of length and time variations of y both are small compared to H^{-1} .

The mean field value at the end of inflation is, from Eqs. (28) and (37),

$$y_x \sim \lambda^{-1/2} H_x, \quad (53)$$

At this field value the characteristic field oscillation frequency is $\omega \sim \lambda^{1/2} y_x \sim H_x$. This means the field starts oscillating at about the time inflation ends, so the field amplitude after inflation decays as $y \sim y_x a_x/a$ until the quadratic part of the potential becomes comparable to the quartic part, at $y \sim y_\mu = \mu \lambda^{-1/2}$. The expansion factor at which this happens is

$$a_\mu/a_x \sim H_x/\mu. \quad (54)$$

The present mean mass density in the y -field, which we are assuming is comparable to the total, is

$$\rho_o \sim z_{\text{eq}} T_o^4 \sim \lambda^{-1} H_x^4 (a_x/a_\mu)^4 (a_\mu/a_o)^3. \quad (55)$$

The mass density at the end of inflation is $\lambda y_x^4/4 \sim \lambda^{-1} H_x^4$ (Eq 53). The present CBR temperature is T_o , and the redshift at equality of mass densities in matter and radiation is $z_{\text{eq}} \simeq 3500$ (for $\Omega_m = 0.3$ and $h = 0.7$).

In the conventional model for reheating it will be sufficient to consider the case where the expansion is radiation-dominated at temperature $T_x \sim (m_{\text{pl}} H)^{1/2}$ at the end of inflation. Then the expansion factor from the end of inflation to the present is $a_o/a_x \sim T_x/T_o$. With Eqs. (54) and (55) we get

$$\mu \sim \lambda z_{\text{eq}} T_o m_{\text{pl}}^3 / T_x^3 \sim 10^5 \lambda T_{14}^{-3} \text{ GeV}, \quad (56)$$

for temperature $T_x = 10^{14} T_{14}$ GeV at the end of inflation. The redshift at which the dark matter starts acting as a massive field is

$$a_o/a_\mu \sim \lambda z_{\text{eq}} (m_{\text{pl}}/T_x)^4 \sim 10^{22} \lambda T_{14}^{-4}. \quad (57)$$

If $\lambda \gg 10^{-14}$ and $T_{14} \sim 1$ the length scales of interest for extragalactic astronomy appear at the Hubble length at redshifts well below this value of a_o/a_μ , and the dynamical behavior of the y -matter is not significantly different from the usual cold dark matter.

In the quintessential picture the mass densities at the end of inflation in gravitationally produced interacting matter and noninteracting matter are

$$\rho_x(\text{matter}) = C H_x^4, \quad \rho_x(\text{dm}) \sim \lambda^{-1} H_x^4. \quad (58)$$

The constant C depends on the matter interactions, as discussed in Section VI-A. Consistency with the standard model for the origin of the light elements requires that the ratio of

these mass densities, $f \sim \lambda C$, be greater than about $f \sim 15$ at the time of light element production. If this condition is violated the model is excluded. If the model is viable we can normalize the parameter constraints to the value of f . The redshift at which the y -field starts acting like a nonrelativistic massive field is

$$z_\mu = a_o/a_\mu \sim f z_{\text{eq}}. \quad (59)$$

The radiation temperature at the end of inflation is $T_x \sim C^{1/4} H_x$, so the expansion factor to the present is $a_o/a_x \sim C^{1/4} H_x/T_o$. With Eq. (54) we have

$$\mu \sim \lambda C^{3/4} z_{\text{eq}} T_o \sim 1 \lambda C^{3/4} \text{ eV}. \quad (60)$$

B. The Effective Jeans Length

In quintessential inflation y starts acting like a massive field at relatively low redshift (Eq. 59), and we have to check the effect on the gravitational growth of clustering of the dark matter. The y -field fluctuations that appear at the Hubble length well after inflation have wavelengths that are much larger than the period of oscillation of y , and the gradient energy density $(\nabla y)^2/2$ thus is strongly subdominant to the kinetic and potential energy densities. We assume dynamical evolution leaves the gradient energy subdominant. We proceed by deriving a virial theorem valid when the field oscillation frequency is much larger than the Hubble parameter, following Ford [12], and use it to estimate the effective pressure from the trace of the stress-energy tensor.

Neglecting the cosmological expansion, the field equation is

$$\ddot{y} - \nabla^2 y + \lambda y^3 + \mu^2 y = 0. \quad (61)$$

The result of multiplying this equation by y , averaging over space, and averaging over a time interval that is much longer than the field oscillation time and much shorter than the cosmological expansion time is

$$\langle \dot{y}^2 \rangle = \langle (\nabla y)^2 \rangle + \lambda \langle y^4 \rangle + \mu^2 \langle y^2 \rangle. \quad (62)$$

With this relation the mean energy density is

$$\langle \rho \rangle = \langle (\nabla y)^2 \rangle + 3\lambda \langle y^4 \rangle / 4 + \mu^2 \langle y^2 \rangle, \quad (63)$$

and the mean of the trace of the stress-energy tensor is

$$\langle T \rangle = \langle \rho \rangle - 3\langle p \rangle = \mu^2 \langle y^2 \rangle, \quad (64)$$

where p is the effective pressure. If the gradient energy is subdominant we have

$$\frac{\langle p \rangle}{\langle \rho \rangle} = \frac{1}{3} \frac{\lambda \langle y^4 \rangle}{\lambda \langle y^4 \rangle + 4\mu^2 \langle y^2 \rangle / 3}. \quad (65)$$

Properties of $y(t)$ considered as a single oscillator with the equation of motion $\ddot{y} = -\lambda y^3$ are discussed by Greene, Kofman, Linde, and Starobinsky [13]. The energy equation for the oscillator is

$$\dot{y}^2/2 + \lambda y^4/4 = \lambda y_o^4/4, \quad (66)$$

where the amplitude is y_o , and we can use this to compute time averages of moments of y . In particular,

$$\langle y^2 \rangle^2 / \langle y^4 \rangle = 48[\Gamma(3/4)/\Gamma(1/4)]^4 \simeq 0.63. \quad (67)$$

When the amplitude is small enough that the quadratic part of the potential dominates,

$$\langle y^2 \rangle^2 / \langle y^4 \rangle = 2/3. \quad (68)$$

In short, we can take it that $\langle y^4 \rangle \sim \langle y^2 \rangle^2$, and we see from Eq. (65) that $\langle p \rangle / \langle \rho \rangle \simeq 1/3$ until $\langle y^2 \rangle \sim \mu^2/\lambda$, at expansion parameter $a \sim a_\mu$. In quintessential inflation this is at redshift $z_\mu \sim fz_{\text{eq}}$ (Eq. 59). At $z < z_\mu$ the ratio varies as $\langle p \rangle / \langle \rho \rangle \propto a^{-3}$, because $\langle y^2 \rangle \propto a^{-3}$ for a massive nonrelativistic field. Thus the effective velocity of sound is $c_s \propto a^{-3/2} \propto t^{-3/4}$ at $z_\mu > a > z_{\text{eq}}$ and $c_s \propto t^{-1}$ at $z < z_{\text{eq}}$. The physical Jeans length $\sim c_s t$ increases as $t^{1/4}$ at $z_\mu \gtrsim z \gtrsim z_{\text{eq}}$ and then approaches a constant. The comoving Jeans length $c_s t/a$ is maximum at z_μ , and the maximum comoving Jeans length referred to the present epoch is

$$L_J \sim t_\mu z_\mu / \sqrt{3} \sim 6/(f\Omega_m h^2) \text{ Mpc}. \quad (69)$$

The world time at redshift z_μ is t_μ , the present matter density parameter is Ω_m , and the present Hubble parameter is h . On comoving scales larger than L_J it is a good approximation to neglect the effect of the field stress on the gravitational evolution of the y -field mass distribution. On smaller scales the dynamical behavior of the field requires a more detailed analysis than is attempted here.

The effective Jeans length in Eq. (69) is smaller than that of a family of neutrinos with mass ~ 30 eV, and may be comparable to the mean distance between large galaxies.

C. The Large-Scale Thermal Background Anisotropy

The parameter λ is bounded by the effect of isocurvature fluctuations in the y -field at the end of inflation on the angular distribution of the thermal background radiation (the CBR). For definiteness we present numerical results for quintessential inflation.

This analysis of the temperature fluctuations on large angular scales uses the simplification that the radiation pressure gradient force has little effect on the mass distribution on the scale of the present Hubble length, so we can imagine that well-separated regions we see at the Hubble length evolve as separate homogeneous cosmological models. In one of these homogeneous models the field value and radiation temperature at the end of inflation are y_x and T_x . By repeating the computation in Section IV-A one finds that the present dark mass density varies with these parameters and the present temperature, T_o , as

$$\rho_o \sim \lambda^{1/2} C^{-3/4} \mu (y_x T_o / T_x)^3. \quad (70)$$

Under the isocurvature initial conditions (and assuming the y -mass density at high redshift is subdominant, as required for light element production), the temperature T_x is nearly homogeneous, the same in all the model universes that represent the evolution of different

regions. Also, the present dominant mass density, ρ_o , is close to homogeneous on the scale of the present Hubble length, because pressure gradient forces cannot generate large-scale curvature fluctuations. Thus the present large-scale CBR anisotropy is

$$\frac{\delta T_o}{T_o} \simeq -\frac{\delta y_x}{y_x} \simeq -\frac{1}{4} \frac{\delta \rho_x}{\rho_x}. \quad (71)$$

This relation also follows in the conventional model for reheating.

We need expansion factors during and after inflation. In quintessential inflation the ratio of the comoving Hubble length now, $x_o = (H_o a_o)^{-1}$, and the Hubble length x_x at the end of inflation is

$$\frac{x_o}{x_x} \sim \frac{H_x a_x}{H_o a_o} \sim C^{-1/4} \frac{T_o}{H_o}. \quad (72)$$

The ratio of the present temperature and Hubble parameter is

$$T_o/H_o \sim e^{67}. \quad (73)$$

When field fluctuations during inflation are being frozen at the comoving scale x_o of the present Hubble length the expansion and Hubble parameters a_p and H_p satisfy

$$H_p a_p \sim H_o a_o \sim C^{1/4} H_x a_x H_o / T_o. \quad (74)$$

These relations with Eq. (29) say the expansion factor from a_p to the end of inflation satisfies

$$a_x/a_p \sim C^{-1/4} (T_o/H_o) \log a_x/a_p. \quad (75)$$

If C is on the order of unity the numerical solution is

$$H_p/H_x = \log a_x/a_p \simeq 72. \quad (76)$$

We have to consider two cases, where the dark matter field departs from near statistical equilibrium and commences classical slow roll before or after ax_o appears at the Hubble length during inflation. The Hubble parameter at the breaking of equilibrium is $H_e \sim \lambda^{-1/2} H_x$ (Eq. 34), so a critical parameter value is

$$\lambda_p = (H_x/H_p)^2 \sim 1 \times 10^{-4}, \quad (77)$$

from Eq (76). If $\lambda \ll \lambda_p$ then we observe in the CBR anisotropy the effect of fluctuations frozen while y was behaving as a classical field that is slightly perturbed by quantum fluctuations. In this case Eqs. (39), (71) to (73) and (76), with the measurement $\delta T_o/T_o \simeq 1 \times 10^{-5}$, imply

$$\lambda \lesssim 1 \times 10^{-6}. \quad (78)$$

This assumes C is on the order of unity in Eq. (72), and unless C is very large its value does not significantly affect the bound on λ . The condition $C \sim f/\lambda$ from Eq. (58) with $f \sim 10$ requires $C \gtrsim 10^7$. This limit is close enough to unity for the purpose of the numerical estimate in Eq. (76).

The bound in Eq. (78) differs from the analysis of Felder, Kofman and Linde [7] by the factor in Eq. (38) that takes account of the classical decay of y from a_p to the end of inflation.

In the other limiting case, $\lambda \gg \lambda_p$, it is convenient to use the expansion of the observed angular distribution of the background temperature in spherical harmonics, with coefficients

$$a_l^m = \int d\Omega Y_l^m \delta T_o / T_o. \quad (79)$$

With Eq (71), and using the addition theorem, $\sum_m Y_l^m(1)Y_l^{-m}(2) = (2l + 1)P_l(\cos \theta_{12})/4\pi$, we can write the mean square value of a multipole moment as

$$\left(\frac{\delta T_l}{T}\right)^2 = \frac{l(2l + 1)}{4\pi} \langle |a_l^m|^2 \rangle = \frac{l(2l + 1)}{4\pi} \int d\Omega P_l(\cos \theta) \xi(x) / 16. \quad (80)$$

In this normalization, $(\delta T_l / T)^2$ is the contribution to the variance of the sky temperature per logarithmic interval of the spherical harmonic index l . The argument of the dark mass correlation function at the end of inflation is $x = 2x_o \sin \theta / 2$, where the present angular size distance x_o back to high redshift is

$$x_o \simeq 3.2(H_o a_o)^{-1}. \quad (81)$$

Here $\Omega_m = 0.3$, we assume zero space curvature, and the present Hubble and expansion parameters are H_o and a_o .

For the dark mass correlation function in Eq. (43) the large-scale anisotropy spectrum is

$$\left(\frac{\delta T_l}{T}\right)^2 = N \frac{l(2l + 1)}{32} \left(\frac{x_x}{x_o}\right)^{0.6\sqrt{\lambda}} \int_{-1}^1 d\mu P_l(\mu) (2 - 2\mu)^{-0.3\sqrt{\lambda}} \lesssim 1 \times 10^{-10}. \quad (82)$$

The observational bound applies at $l \lesssim 30$. We have written $x_x/x = (x_x/x_o)(x_o/x)$; the second factor produces the last factor in the integrand. The solution to this equation at $\lambda \ll 1$ is not relevant because the limit in Eq. (78) applies. In the solution at λ close to unity the integral is of order unity and the value of the integral and the factor N in the primeval mass correlation function do not much matter because the sensitive function is $(x_x/x_o)^{0.6\lambda}$. We have

$$\lambda \gtrsim 0.3. \quad (83)$$

In the conventional reheating picture $\log a_x/a_p$ is about ten percent smaller. To the accuracy of our estimates the constraints on λ are the same.

VI. DISCUSSION

We comment first on issues of consistency and reasonableness of the noninteracting dark matter picture within conventional and quintessential endings of inflation, and then take note of some observational challenges.

A. Theoretical Issues

For the purpose of exploring a simple example of dark matter that interacts only with itself and gravity we have considered a quartic plus quadratic self-interaction potential. This functional form has the arguably attractive feature that one can choose constant coefficients that imply an interesting present mean dark mass density and CBR anisotropy. We are not competent to say whether other models for a self-interaction potential would be more plausible from the point of view of fundamental physics or would produce dark matter candidates with more interesting properties.

In the quartic plus quadratic potential the isotropy of the CBR requires that the dimensionless parameter λ be in the narrow range

$$0.3 \lesssim \lambda \lesssim 1, \quad (84)$$

or else be quite small,

$$10^{-6} \gtrsim \lambda \gg \lambda_\phi \lesssim 10^{-14}. \quad (85)$$

The last bound is the condition on the adiabatic density fluctuations produced by the inflaton. The upper limit in Eq. (84) is the condition that the potential be safe from significant renormalization (Eq. 4). We know of no reason to think either range of values of λ is particularly attractive within fundamental physics, though it is to be hoped that input from this direction eventually will be a factor in the completion of a satisfactory theory of structure formation.

In a recent paper Felder, Kofman and Linde [7] (hereafter FKL) raise a number of issues relevant to our analysis. They note that scalar fields whose particles are produced gravitationally at the end of inflation could end up dominating the energy density, thus assuming the role of the inflaton. This could indeed happen if the self-couplings of some of these fields in quartic potential models were smaller than that of the inflaton. One sees from Eqs. (35) and (37) that the ratio of energy densities in the inflaton and a field with self-coupling λ_j in the quartic model is

$$\rho_j/\rho_\phi = \lambda_\phi/\lambda_j. \quad (86)$$

Thus consistency within this model requires $\lambda_j \gg \lambda_\phi$. Since the interacting scalar fields of the quintessential model [6] are usual spin-0 particles, like the Higgses that interact with gauge fields, their couplings are not expected to be particularly small. The inflaton coupling, on the other hand, is required to be small [Eq.(85)], and there does not seem to be a problem in meeting the conditions on λ_j .

FKL note that the λ_j are also constrained by the condition that the isocurvature fluctuations produced by the scalar fields not violate the CBR isotropy. The point is valid when some of the fields represent stable non-interacting massive particles. Indeed, we find that the range $10^{-6} \ll \lambda_j \lesssim 0.3$ is excluded for noninteracting dark matter.⁴

⁴Our larger lower bound on λ_j seems to be mainly due to the correction for the decay of field fluctuations in Eq (38). Our larger allowed range applies when the equilibrium between quantum excitations and classical decay of the dark matter field persists to close to the end of inflation, a case FKL do not consider.

Interacting scalar fields, such as the Higgses, also are produced with inhomogeneous distributions at the end of inflation. These particles interact by the usual decay, annihilation and production processes that produce local thermal equilibrium. In the absence of particle number conservation laws, this local thermal equilibrium is fully described by a single function of position — the temperature or the mass density. Apart from the adiabatic perturbations from the inflaton the model predicts negligible spacetime curvature fluctuations at the end of inflation. This means the matter density fluctuations correspond to fluctuations in the local starting times of cosmological expansion with universal values of the cosmological parameters. If all matter interacts and relaxes to local thermal equilibrium the result at the present time is an unacceptably homogeneous universe. If a dark matter component does not interact with the rest of the matter, the possibility considered in this paper, fluctuations in composition, which is to say isocurvature fluctuations, remain. There may also be adiabatic curvature fluctuations from the inflaton, of course. Either or both could act as seeds for structure formation.

FKL also point out that the moduli problem is more severe than in the conventional picture for reheating. Moduli are light scalar fields with only gravitational-strength coupling to ordinary matter. They necessarily arise in supergravity models and superstring theories. The curvature correction generally makes the effective potential of a modulus χ during inflation different from at late times, the minima of the two potentials tending to be displaced by $\Delta\chi \sim m_{\text{pl}}$. Thus, after inflation one has a nearly homogeneous field χ with $\rho_\chi \sim m_\chi^2(\Delta\chi)^2 \sim m_\chi^2 m_{\text{pl}}^2$. The mass m_χ is determined by the supersymmetry breaking scale η_{SUSY} ,

$$m_\chi \sim \eta_{SUSY}^2/m_{\text{pl}}. \quad (87)$$

In models with gravity-mediated supersymmetry breaking, $\eta_{SUSY} \sim 10^{11}$ GeV and $m_\chi \sim 10^3$ GeV. The main problem with the moduli is that they may decay very late. With $m_\chi \sim 10^3$ GeV, the lifetime is

$$\tau \sim m_{\text{pl}}^2/m_\chi^3 \sim 10^5 \text{ s}, \quad (88)$$

so one runs into problems with nucleosynthesis and with photodissociation and photoproduction of light elements by the decay products of χ [14].

There are two commonly discussed possible solutions to the moduli problem. First, a short period of secondary inflation could dilute the moduli [15]. This naturally occurs in “thermal” inflation [16], but seems unlikely to be effective in quintessential inflation, where the relative density of the moduli is much higher than in the conventional picture, as pointed out by FKL. Second, the minima of $V(\chi)$ during and after inflation may coincide due to some symmetry [17–19]. In this case moduli are produced only gravitationally, like other light scalars, and have density $\rho_\chi \sim H^4$ at the end of inflation. The density of matter in standard inflation is $\rho_m \sim m_{\text{pl}}^2 H^2$, and $\rho_\chi/\rho_m \sim H^2/m_{\text{pl}}^2$ is small enough to solve the moduli problem. However, in quintessential inflation $\rho_m \sim H^4$ and $\rho_\chi/\rho_m \sim 1$, which is clearly too high.

There are other ways out, however. During inflation, moduli typically acquire masses [17,20] $m_\chi \sim \beta H$ with $\beta \gtrsim 1$, and it is conceivable that $\beta \gg 1$ [17,21]. The gravitational production of moduli would then be exponentially suppressed. Moduli can also develop non-perturbative potentials, independent of supersymmetry breaking [22]. Their mass can

then be large enough that the lifetime in Eq. (88) is $\tau \ll 1s$. Assuming coincident minima of $V(\chi)$ during and after inflation, this would eliminate the problem with light elements. If the moduli decay prior to baryogenesis, then the relaxation to thermal equilibrium eliminates the isocurvature perturbation associated with the inhomogeneous primeval local ratio of entropy density to the number density of modulus quanta. Otherwise, the isocurvature perturbation survives in the form of an inhomogeneous ratio of the baryon and photon number densities and can later play a role in structure formation.

Another possibility is that the supersymmetry breaking scale could be much smaller than 10^{11} GeV; in some models it can be as low as the electroweak scale [23]. The moduli would then be very light, their lifetime would be much greater than the present age of the universe, and problems with nucleosynthesis would not arise. (Here we still assume coincident minima and also that the moduli develop masses $\sim H$ during inflation).

There is a related issue for gravitinos. The lower energy density at the end of inflation in the quintessential picture reduces thermal gravitino production but increases the problem of gravitational production, as FKL note. Apart from potential energy terms the gravitino obeys a conformally invariant field equation [24]. If during inflation the gravitino had a substantial effective mass, the gravitino energy density from gravitational particle production could be unacceptable in quintessential inflation. We are not aware that the effective mass has to be this large, however.

The moduli and gravitino quanta are close approximations to the proposed noninteracting dark matter, but with potentially unacceptable production of mass density. This is a challenge, but within the not inconsiderable uncertainties of a supersymmetric theory that has not yet been fully specified the challenge does not seem serious enough to discourage further exploration of the picture.

We note finally that the density of matter produced in quintessential inflation can be substantially higher than our original estimate in Ref. [6]. The quanta of spin-0 fields χ_j produced due to the change in the expansion law at the end of inflation have wavelength $\sim H_x^{-1}$ and energy density $\rho_j^{(s)} \sim H_x^4$. In addition to these short-wavelength quanta, there is also a nearly homogeneous component of χ_j . The classical solution (37) always applies at the end of inflation, and the energy of the homogeneous component follows as in Eq. (58),

$$\rho_j^{(h)} \sim (\lambda_\phi^2/\lambda_j)m_{\text{pl}}^4 \sim \lambda_j^{-1}H_x^4, \quad (89)$$

where $H_x \sim \lambda_\phi^{1/2}m_{\text{pl}}$ is the expansion rate at the end of inflation. We see that $\rho_j^{(h)} \gg \rho_j^{(s)}$ for small λ_j . For ordinary (interacting) matter fields, the homogeneous component decays and thermalizes, just like the short-wavelength quanta. We note also that this enhancement of the energy density in the homogeneous component disappears if the fields χ_j develop masses $m_j \sim H$ during inflation. In this case the original estimate of [6], $\rho_j \sim H_x^4$, is still valid, for $\lambda_j < 1$, because the quartic term is small compared to the quadratic part of the potential.

B. Observational Issues

Previous examples of noninteracting dark matter [25], [26] postulate a quadratic self-interaction potential with a time-variable mass. These are CDM models, where the CDM is defined as matter that has had negligible pressure since appearance at the Hubble length

of all length scales of astrophysical interest. The two-field CDM model in [26] could be adjusted to fit the spectrum $\delta T_l/T$ of angular fluctuations of the thermal background, to the accuracy of the measurements then available, but at $l \sim 50$ the model power is a factor of two above the new Python [27] result. Bridging this gap would require even greater contrivance. This isocurvature CDM model thus does not seem to be viable, but it does offer a useful reference for a first assessment of observational tests of the quartic plus quadratic self-interaction model.

In the isocurvature CDM model the primeval distribution of the radiation is much smoother than that of the CDM because the mean mass density in the CDM is much smaller. With the quartic potential considered here the dark matter approximates a fluid with the equation of state of the radiation until the redshift approaches z_{eq} (Eq. 59). This means a given primeval isocurvature fluctuation $\delta\rho_y/\rho_y$ in the dark matter distribution produces a much larger primeval perturbation to the distribution of the radiation than for CDM. The effect on the fluctuation spectrum of the CBR on angular scales below the limit of application of Eq. (82) remains to be computed.

In the isocurvature CDM model the primeval mass distribution is $\rho \propto y(\mathbf{x})^2$, with y a random Gaussian process, and the non-Gaussian mass density fluctuations in this model may violate the measured skewness and kurtosis of the large-scale fluctuations of galaxy counts [10]. The numerical realizations in Fig. 2 indicate that in the quartic potential model the skewness of the primeval mass distribution is a factor of about 3 smaller than in the case $\rho \propto y^2$. Again, the effect on the observational constraint may be worth investigating.

In quintessential inflation the dynamical behavior of the y -field would be an important factor in the formation of the first generations of structure (Eq. 69). Khlebinkov and Tkachev [28] present numerical simulations of the three-dimensional behavior of a scalar field with quartic self-interaction potential, in connection with the dynamics of reheating in conventional inflation. They find a marked tendency for the growth of field fluctuations on ever smaller scales. The qualitative effect is easily understood: where the field value $|y|$ is larger than average the field oscillation frequency is larger, and the frequency differences at different positions produce growing field gradients. Our preliminary numerical experiments in one space dimension plus time suggest the growing field gradients produce energy fluxes that redistribute energy and the space distribution of field oscillation frequencies. This tends to unwind the field gradients through substantial parts of space, while leaving localized regions with relatively large field gradient energy density. The effect is curious enough that further study would be at least intellectually interesting, and it is conceivable that it adds an interesting complication to the observed growth of structure on the scale of galaxies.

Finally, we return to our opening remark, that it may be useful to complement the growing observational basis for a theory of structure formation with surveys of the options available within conventional physics. It is natural to consider simplest possibilities first, but prudent to bear in mind the possibility of complications. An example is the evidence that the density parameter in matter capable of clustering on scales much smaller than the Hubble length is significantly below unity [29]. If this were valid it would mean that the large-scale nature of the universe is not as simple as we could imagine within conventional physical ideas, a result that could hardly be described as surprising in light of the ample opportunities for complexity in the physical universe. We arrived at a simple model for structure formation, adiabatic CDM, fifteen years ago, after abandoning a few even simpler

ideas. In the present paper we have considered a class of dark matter candidates whose properties could be considerably more complicated than cold dark matter, and the observational predictions much harder to work out. On the other hand, the picture does not seem unnatural: possibly some of the fields gravitationally produced by inflation are unable to thermalize with ordinary matter; perhaps such fields end up with an observationally interesting dark mass density; perhaps their irregular primeval distributions are a significant factor in seeding the gravitational growth of structure.

VII. ACKNOWLEDGMENTS

We thank Lev Kofman for an advance copy of his recent paper with Felder and Linde [7]; it helped improve our paper. We have also benefitted from discussions with Gia Dvali, Massimo Giovannini, Andrei Gruzinov, Lev Kofman, Andrei Linde, Alison Peebles, David Spergel, and Paul Steinhardt. This research was supported in part at the Institute for Advanced Study by the Alfred P. Sloan Foundation and at Tufts University by the National Science Foundation.

VIII. APPENDIX A. CALCULATION OF TWO- AND THREE-POINT FUNCTIONS

To calculate the two- and three-point correlation functions in de Sitter space, it will be convenient to introduce the conditional probability $\Pi(y, t|y_0, t_0)$ for the field to have value y at time t , given that it had value y_0 at time t_0 at the same co-moving position. This probability satisfies the Fokker-Planck equation (7) with the initial condition

$$\Pi(y, t_0|y_0, t_0) = \delta(y - y_0), \quad (90)$$

and can be expressed as [30]

$$\Pi(y, t|y_0, t_0) = e^{-v(y)+v(y_0)} \sum_{k=0}^{\infty} \Phi_k(y)\Phi_k(y_0)e^{-\Lambda_k(t-t_0)}. \quad (91)$$

Here,

$$v(y) \equiv \frac{4\pi^2}{3H^4}V(y), \quad (92)$$

and $\Phi_k(y)$ form a complete orthonormal set of eigenfunctions of the equation

$$\left[-\frac{\partial^2}{\partial y^2} + v'(y)^2 - v''(y) \right] \Phi_k(y) = \frac{8\pi^2\Lambda_k}{H^3}\Phi_k(y). \quad (93)$$

The eigenvalues Λ_k are non-negative, with the smallest eigenvalue $\Lambda_0 = 0$ corresponding to

$$\Phi_0(y) = N^{-1/2}e^{-v(y)}, \quad (94)$$

with

$$N = \int_{-\infty}^{\infty} e^{-2v(y)} dy. \quad (95)$$

Note that $\Phi_0(y)$ is related to the ‘‘equilibrium’’ distribution function (8),

$$P_0(y) = \Phi_0^2(y). \quad (96)$$

we shall assume that the eigenfunctions are ordered so that $0 < \Lambda_1 < \Lambda_2 < \dots$. For a purely quartic potential [4],

$$\Lambda_1 = 0.0889\lambda^{1/2}H, \quad \Lambda_2 = 0.289\lambda^{1/2}H. \quad (97)$$

Let us now consider two co-moving positions \mathbf{x}_1 and \mathbf{x}_2 separated by a distance $ax = a|\mathbf{x}_1 - \mathbf{x}_2| \gg H^{-1}$ at some moment $t = 0$. These positions were within each other’s horizons prior to the time

$$t_a = -H^{-1} \ln(Hax). \quad (98)$$

For $t < t_a$, the values of y at \mathbf{x}_1 and \mathbf{x}_2 are essentially the same. Hence, the probability for y to take a value y_1 at \mathbf{x}_1 and a value y_2 at \mathbf{x}_2 at time $t = 0$ can be expressed as [4]

$$P_2[y_1(\mathbf{x}_1), y_2(\mathbf{x}_2)] = \int \Pi(y_1, 0|y_a, t_a)\Pi(y_2, 0|y_a, t_a)P_0(y_a)dy_a, \quad (99)$$

where $P_0(y)$ is the equilibrium distribution (96). The equal-time two-point correlation function for y^n is given by

$$\begin{aligned} \langle y^n(\mathbf{x}_1, 0)y^n(\mathbf{x}_2, 0) \rangle &\equiv \langle y_1^n y_2^n \rangle = \int_{-\infty}^{\infty} dy_1 dy_2 y_1^n y_2^n P_2[y_1(\mathbf{x}_1), y_2(\mathbf{x}_2)] \\ &= N^{-1} \sum_{k=0}^{\infty} A_{(n)k}^2 (Hax)^{-2\Lambda_k/H}, \end{aligned} \quad (100)$$

where

$$A_{(n)k} = \int_{-\infty}^{\infty} y^n e^{-v(y)} \Phi_k(y) dy \quad (101)$$

and we have used Eqs. (91), (98), (99) and the orthonormality of the functions $\Phi_k(y)$. The mode functions $\Phi_k(y)$ are even functions of y for k even and odd functions of y for k odd ($\Phi_k(y)$ has k nodes), and it is clear from Eq. (101) that $A_{(n)k}$ are non-zero only when n and k are both even or both odd.

The first term in the series (100) is

$$N^{-1} A_{(n)0}^2 = \langle y^n \rangle^2, \quad (102)$$

and thus the reduced two-point function,

$$c_n(x) = \langle y_1^n y_2^n \rangle - \langle y^n \rangle^2, \quad (103)$$

is given by the same series starting with $k = 1$. The asymptotic behavior of $c_n(x)$ at large x is determined by the first term in that series. For odd values of n ,

$$c_n(x) \approx N^{-1} A_{(n)1}^2 (Hax)^{-2\Lambda_1/H}. \quad (104)$$

For even values of n , $A_{(n)1} = 0$ and

$$c_n(x) \approx N^{-1} A_{(n)2}^2 (Hax)^{-2\Lambda_2/H}. \quad (105)$$

Eqs. (11), (12) of Section III follow immediately from these relations.

Quite similarly, the three-point function can be expressed as

$$\langle y_1^4 y_2^4 y_3^4 \rangle = \int dy_1 dy_2 dy_3 y_1^4 y_2^4 y_3^4 P_3[y_1(\mathbf{x}_1), y_2(\mathbf{x}_2), y_3(\mathbf{x}_3)]. \quad (106)$$

Assuming that $\mathbf{x}_1, \mathbf{x}_2, \mathbf{x}_3$ form an equilateral triangle of side ax , the probability distribution P_3 can be written as

$$P_3[y_1, y_2, y_3] = \int \Pi(y_1, 0|y_a, t_a) \Pi(y_2, 0|y_a, t_a) \Pi(y_3, 0|y_a, t_a) P_0(y_a) dy_a, \quad (107)$$

Combined with equations (106),(91),(98), this gives

$$\langle y_1^4 y_2^4 y_3^4 \rangle = N^{-1} \sum_{k,l,m=0}^{\infty} A_{(4)k} A_{(4)l} A_{(4)m} (Hax)^{-(\Lambda_1+\Lambda_2+\Lambda_3)/H} \int \Phi_k(y) \Phi_l(y) \Phi_m(y) e^{v(y)} dy. \quad (108)$$

Once again, it is easily understood that the reduced three-point function (20) is given by the same series with the summation starting at $k, l, m = 2$. The leading term at large x is

$$\xi_3(x) \approx N^{-1} A_{(4)2}^3 C (Hax)^{-3\Lambda_2/H}, \quad (109)$$

where

$$C = \int_{-\infty}^{\infty} \Phi_2^3(y) e^{v(y)} dy. \quad (110)$$

From (105) and (109) we find that at large x

$$\xi_3(x)/\xi_2^{3/2}(x) \approx N^{1/2} C, \quad (111)$$

independent of x .

REFERENCES

- [1] D. J. Eisenstein, W. Hu, and M. Tegmark, *Astrophys. J.* in press (astro-ph/9807130), and references therein.
- [2] A. Vilenkin, *Phys. Rev.* **D27**, 2848 (1983).
- [3] A.A. Starobinsky, in *Field Theory, Quantum Gravity and Strings*, ed. by H.J. de Vega and N. Sanchez (Springer, Heidelberg, 1986).
- [4] A. A. Starobinsky and J. Yokoyama, *Phys. Rev. D.* **50**, 6357 (1994).
- [5] L. Kofman and A.D. Linde, *Nucl. Phys.* **B282**, 555 (1987).
- [6] P. J. E. Peebles and A. Vilenkin, *Phys. Rev.* **D59**, 063505 (1999).
- [7] G. Felder, L. Kofman and A. D. Linde, hep-ph/9903350.
- [8] The one-loop effective potential for the model (1) in de Sitter space was calculated in Ref. [9]. The condition (4) is obtained by requiring that the one-loop correction is negligible for $y^2 \lesssim \langle y^2 \rangle \sim \lambda^{-1/2} H^2$, where the expectation value $\langle y^2 \rangle$ is taken in the de Sitter-invariant state (see section III).
- [9] A. Vilenkin, *Nucl. Phys.* **B226**, 504 (1983).
- [10] E. Gaztañaga and P. Fosalba, *Monthly Notices Royal Astronomical Society* **301**, 534 (1998); M. White, astro-ph/9811227; J. A. Frieman and E. Gaztañaga, astro-ph/9903423.
- [11] A. D. Linde, *Particle Physics and Inflationary Cosmology* (Harwood Academic, Chur, 1990).
- [12] L. H. Ford, *Phys. Rev. D* **35**, 2955 (1987).
- [13] P. B. Greene, L. Kofman, A. Linde, and A. A. Starobinsky, *Phys. Rev. D* **56**, 6175 (1997).
- [14] Ellis, J. *et.al.*, *Nucl.Phys.* **B373**, 399 (1992).
- [15] L. Randall and S. Thomas, *Nucl.Phys.* **B449**, 229 (1995).
- [16] D. H. Lyth and E. D. Stewart, *Phys. Rev. Lett.* **75**, 201 (1995).
- [17] G. Dvali, *Phys. Lett.* **B355**, 78 (1995).
- [18] M. Dine, L. Randall and S. Thomas, *Phys. Rev. Lett.* **75**, 398 (1995).
- [19] T. Damour and A. Vilenkin, *Phys. Rev.* **D53**, 2981 (1996)
- [20] M. Dine, W. Fischler and D. Nemeschansky, *Phys. Lett.* **B136**, 169 (1984).
- [21] A.D. Linde, *Phys. Rev.* **D53**, 4129 (1996).
- [22] G. Dvali and Z. Kakushadze, *Phys. Lett.* **B417**, 50 (1998).
- [23] I. Antoniadis, S. Dimopoulos and G. Dvali, *Nucl. Phys.* **B516**, 70 (1998).
- [24] L.P. Grishchuk and A.D. Popova, *Zh. Eksp. Teor. Fiz.* **77**, 1665 (1979) [*Sov. Phys. JETP* **50**, 835 (1979)].
- [25] A. Linde and V. Mukhanov, *Phys. Rev.* **D56**, 535 (1997).
- [26] P. J. E. Peebles, *Astrophys. J.* **510**, 523 (1999); P. J. E. Peebles, *Astrophys. J.* **510**, 523 (1999).
- [27] K. Coble *et al.*, preprint (astro-ph/9902195).
- [28] S. Yu. Khlebnikov and I. I. Tkachev, *Phys. Rev. Lett.* **77**, 219 (1996).
- [29] N. A. Bahcall and X. Fan, *Proc. N. A. S. USA* **95**, 5956 (1998); P. J. E. Peebles, *Phil. Trans. R. Soc. London. A* **357**, 21 (1999).
- [30] H. Risken, *The Fokker-Planck Equation*, Springer-Verlag, Berlin, 1989.

FIGURES

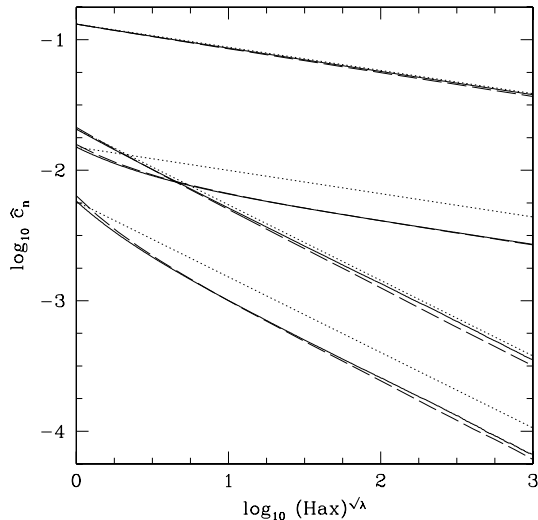


FIG. 1. Numerical realizations of the reduced two-point correlation functions of powers n of the field y (Eq. 11), for $n = 1, 2, 3$, and 4 from top to bottom at the left-hand side of the figure. The dotted lines have the intercept at zero separation and the slope at large separation of the Fokker-Planck approximation (Eqs. 10 to 12). The curves are averages across numerical realizations of the random process for $\lambda = 0.1$ (dashed lines) and $\lambda = 1 \times 10^{-4}$ (solid lines). The correlation functions and the separation are scaled to remove the dependence on λ and H (Eq. 17).

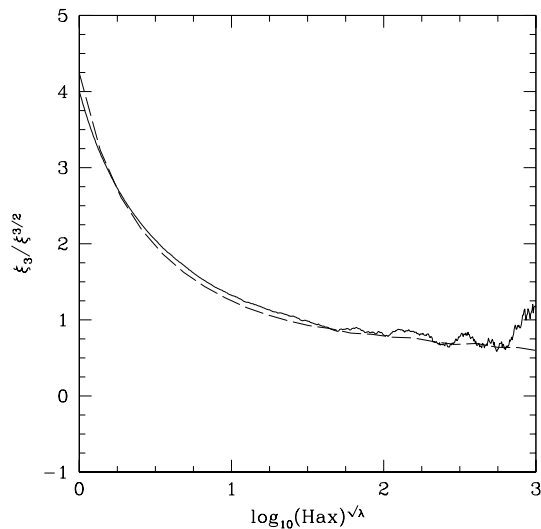


FIG. 2. The reduced three-point correlation function ξ_3 for equilateral triangles scaled by the two-point function ξ evaluated at the length of the side of the triangle for $\lambda = 1 \times 10^{-4}$ (solid line) and $\lambda = 0.1$ (dashed line). In the Fokker-Planck approximation the ratio plotted on the ordinate is constant on scales much larger than the coherence length aR_c .

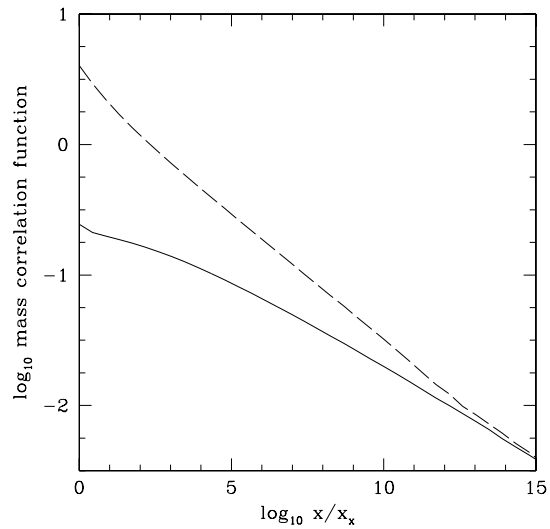


FIG. 3. Numerical realizations of dark mass two-point correlation functions at the end of inflation for the de Sitter equilibrium state (dashed line) and the rolling Hubble parameter in Eqs (45) and (47). The self-coupling parameter in the dark mass potential is $\lambda = 0.1$